

# REVIEW OF PREDICTIONS OF HARD PROBES IN $p+\text{Pb}$ COLLISIONS AT $\sqrt{s_{NN}} = 5.02$ AND 8.16 TeV AND COMPARISON WITH DATA

R. Vogt

*Lawrence Livermore National Laboratory, Livermore, CA 94551, USA*  
*Physics Department, University of California, Davis, CA 95616, USA*



Predictions have been compiled for the  $p+\text{Pb}$  LHC runs, focusing on production of hard probes in cold nuclear matter. These predictions were first made for the  $\sqrt{s_{NN}} = 5.02$  TeV  $p+\text{Pb}$  run and were later compared to the available data. A similar set of predictions were published for the 8.16 TeV  $p+\text{Pb}$  run. A selection of the predictions are reviewed here.

Presented at EDS Blois 2019  
 The 18th Conference on Elastic and Diffractive Scattering  
 Quy Nhon, Vietnam,  
 June 2328, 2019

## 1 Introduction

This proceedings paper covers some of predictions for the production of hard probes in minimum bias  $p+\text{Pb}$  collisions in the  $\sqrt{s_{NN}} = 5.02$  and 8.16 TeV runs in 2012 and 2016. The predictions at 5.02 TeV were presented in Ref. [1] with a follow up comparison to the data published so far in Ref. [2]. The predictions for 8.16 TeV were compiled in Ref. [3]. The focus was on hard probes because they are high mass or high energy probes and therefore calculable in perturbative QCD. Due to their higher energy scales, they are produced early in the history of the collision, thus carrying information about the state of the system when they were produced. This is especially true of probes such as hard photons, Drell-Yan dileptons and massive gauge bosons which are unaffected by the strong interaction and thus travel through the medium without interaction. They are thus especially important for differentiating the parton distributions in a nucleus from those in a proton.

The two proton-lead runs at the LHC have provided access to a system that is intermediate to the “vacuum” of proton-proton collisions and the hot dense quark-gluon plasma produced in heavy-ion collisions such as  $\text{Pb}+\text{Pb}$ . There have been important comparisons between  $p+\text{Pb}$  and  $p + p$  collisions to determine the level of “cold nuclear matter” effects, the modifications

of hard probes due to the nuclear medium without a quark-gluon plasma, while comparisons between  $p$ +Pb and Pb+Pb collisions differentiates between cold and “hot” nuclear matter. While the calculations discussed here were made for minimum bias collisions, with a relatively low multiplicity, it has been noted that the highest multiplicity  $p + p$  and  $p$ +Pb collisions share some characteristics with heavy-ion events. For a more detailed discussion of this and additional references, see Ref. [3].

Due to the lack of space, there can be only a minimal discussion of the predictions. The fewest required references are included here, in particular any new data since the publication of the compilations in Refs. [1–3]. Please see the compilations themselves for full details, along with references to the original work.

The focus here is on new results. Therefore, under quarkonium and heavy flavor, new data on  $\Upsilon$  [4, 5] from ALICE and LHCb and  $B$  mesons from LHCb [6, 7] modifications at 8.16 TeV are compared to predictions. New modifications of the nuclear parton densities based on the dijet and gauge boson data, the EPPS16 [8] set, is discussed, followed by a discussion of these data at 5.02 TeV. Finally, top quark production, measured in collisions involving nuclei for the first time, is also discussed.

## 2 $\Upsilon$ and $B$ meson modifications

Quarkonium and open heavy flavor production were presented together in the compilations. In Refs. [1–3],  $J/\psi$  production was calculated both in approaches employing collinear factorization and saturation approaches. Since  $\Upsilon$  results are shown here, only results assuming collinear factorization are shown because the  $\Upsilon$  mass scale is too high for saturation effects to be relevant.

The calculations shown in Fig. 1 are predominantly from two sources, both of which focus on nuclear PDFs and are shown as functions of transverse momentum,  $p_T$ , and rapidity,  $y$ . An additional calculation, based on energy loss, without any nPDF modification, is only shown as a function of rapidity. The calculations labeled EPS09NLO CEM are made in the color evaporation model, CEM, at next-to-leading order, NLO, with the EPS09 nPDF set using  $b$  quark masses and scales from a fit to  $b\bar{b}$  cross section data [9]. The calculations labeled EPS09NLO, EPS09LO and nCTEQ [11] were made by Lansberg and Shao [10] employing a data-driven approach featuring the  $gg$  channel only with parameterized amplitude and coefficients that can be fit to  $p + p$  data. Note that the EPS09NLO calculations are similar in the two approaches but not identical, the CEM calculation is a complete NLO calculation, with all production channels include and no a priori assumption that the factorization and renormalization scales need to be equal to the mass. The energy loss calculation by Arleo, shown as a function of rapidity, also assuming a parameterized fit to the  $p + p$  cross section. The energy loss is implemented by a shift of the rapidity in  $p$ +Pb collisions relative to  $p + p$  collisions.

The trends of all the nPDF calculations are similar. At forward rapidity, there is a depletion of the nuclear modification factor,  $R_{p\text{Pb}}$ , at low  $p_T$ . (Here, and in the rest of this paper,  $R_{p\text{Pb}}$  is effectively calculated as the cross section per nucleon in  $p$ +Pb collisions relative to the  $p + p$  cross section in the same kinematic range.) The depletion goes away at higher  $p_T$  due to the nPDF scale evolution. As a function of rapidity, the calculations show antishadowing at negative rapidity, larger momentum fractions,  $x$ , in the lead nucleus, and a depletion at forward rapidity, where the  $x$  in the lead nucleus is low. There are large uncertainty bands reflecting the error sets of the nPDF global analyses. Because the energy loss calculation does not assume any difference between the gluon PDFs in the proton and the lead nucleus, the only uncertainty is due to that on the energy loss parameter, resulting in a narrow range of energy loss predictions. All of the calculations are within the uncertainties of the data from ALICE [4] and LHCb [5], shown in the black and red points respectively.

The same data driven parameterization, albeit with different parameter values, are also shown in Fig. 2 for  $B^+$  production in 8 TeV collisions. The trends are the same as those seen

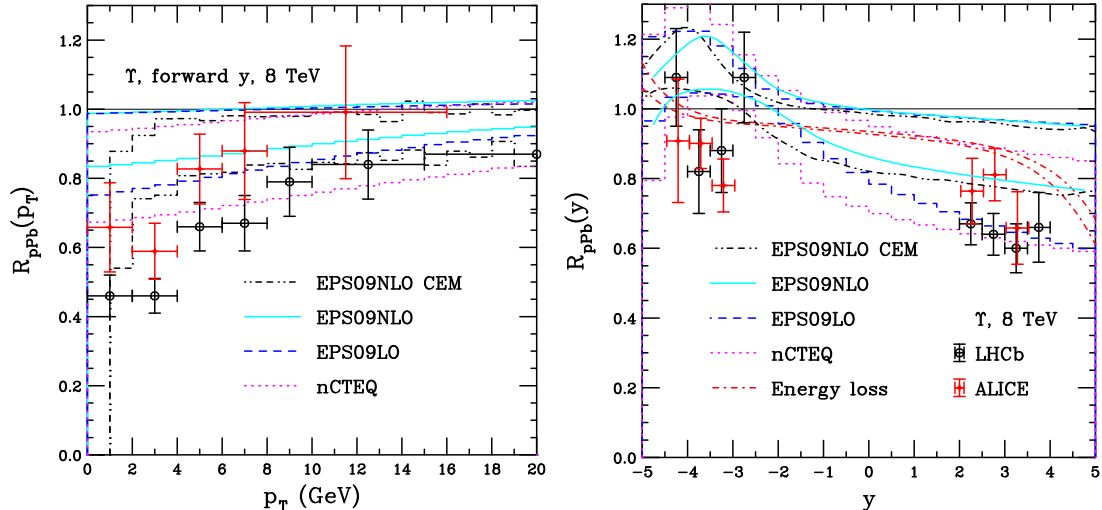


Figure 1 – The nuclear suppression factor  $R_{pPb}$  for  $\Upsilon$  at  $\sqrt{s} = 8.16$  TeV as a function of  $p_T$  at forward rapidity (left) and as a function of rapidity (right). The EPS09 NLO results in the CEM (dot-dot-dash-dashed black) are shown with Lansberg and Shao’s data-driven fits with EPS09 NLO (solid cyan), EPS09 LO (dashed blue) and nCTEQ (dotted magenta). On the right hand side, an energy loss calculation by Arleo (dot-dashed red curve) is also shown. The LHCb [5] and ALICE [4] data are shown by the black and red points respectively. Modified from Ref. [3].

as a function of  $p_T$  and  $y$  for  $\Upsilon$  production.

Two additional predictions are shown for  $B$  mesons. The calculations of Vitev and collaborators, see Refs. [2,3] for details, labeled as ‘Cronin’ and ‘eloss’ on  $R_{pPb}(p_T)$ , also include dynamical shadowing, different from the nPDF parameterizations. The Cronin effect results in  $k_T$  broadening and thus an enhancement at low  $p_T$ , rather than a depletion due to the nPDF only calculations by Lansberg and Shao. The inclusion of energy loss in the calculations weakens the low  $p_T$  enhancement. The calculations shown as a function of rapidity also include a prediction from HIJING ++ a revised version of the general purpose HIJING simulation of heavy-ion collisions, shown as points in the figure.

LHCb data on non-prompt  $J/\psi$ , those from  $B$  meson decays, as well as data where the  $B^+$  is reconstructed [6,7]. The data are most consistent with the nPDF calculations. The calculations assuming Cronin and energy loss are more inconsistent with the data since they do not show any enhancement at low  $p_T$ . HIJING ++ is too high at negative rapidity but is consistent with the calculations at forward rapidity.

These results, with the large nPDF uncertainties, highlight the need for updated nPDF sets, especially in further constraining the gluon nPDFs.

### 3 Modifications of the Parton Densities in Nuclei

One physics outcome from the 5 TeV  $p$ +Pb run was the new set of nuclear parton distribution functions (nPDFs) by Eskola and collaborators, EPPS16 [8]. This set is the first to include the LHC data, specifically that of  $W^\pm$  and  $Z^0$  production from CMS [14,15] and ATLAS [16] as well as the dijet data from CMS [17]. These data could be included in the global analyses because they were all forward-backward asymmetry data and do not rely on a  $p+p$  baseline at the same energy. They also added, for the first time for the Eskola *et al.* sets, neutrino deep-inelastic scattering data.

Incorporating the LHC and neutrino data into the analysis allowed more detailed flavor separation for the quark sets. In particular, the LHC data allowed them to increase the fit range in momentum fraction,  $x$ , and factorization scale,  $Q^2$ , to regions heretofore unavailable in lepton-nucleus collisions. Unfortunately, even with the dijet data from CMS, the gluon distribution in

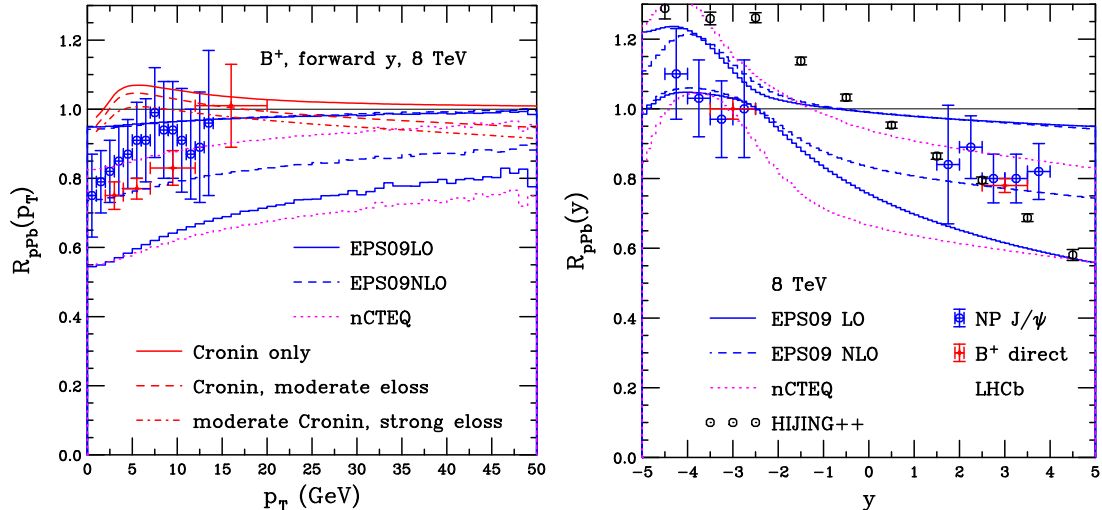


Figure 2 – The calculated  $R_{pPb}$  for the LHC non-prompt  $J/\psi$  [6] and  $B^+$  [7] data are compared with with EPS09 LO (blue), EPS09 NLO (cyan) and nCTEQ (red) as a function of  $p_T$  at forward rapidity (left) and as a function of rapidity (right). Also shown as a function of  $p_T$  is a prediction with  $k_T$  broadening (Cronin) and energy loss while a prediction of HIJING ++ is shown as a function of rapidity. Modified from Ref. [3].

the nucleus, particularly at low  $x$  and moderate  $Q^2$ , is still not well constrained.

These sets were not yet available at the time most of the predictions for Ref. [3] were collected except for the top quark predictions, shown later. However, it is worth noting that the central EPPS16 set gives results quite similar to those calculated with EPS09 NLO [20]. The largest change, for gluon-dominated processes, is the increase in the uncertainty band due to the increased number of parameters required for flavor separation and the relaxing of some previous constraints. See Ref. [8] for details and comparison to the 5.02 TeV  $p$ +Pb data included in the global analysis.

One might expect further global analyses of the nuclear parton densities after more data, especially from the 8.16 TeV run become available. At a given  $p_T$ , the  $x$  value probed in a hard scattering process is a factor of 0.62 smaller at 8.16 TeV than 5.02 TeV. In addition, the higher energy allows a somewhat broader reach in rapidity so that some processes, such as  $Z^0$  production at LHCb, see the discussion in Ref. [2], measured near the edge of phase space, can expect higher statistics and perhaps high enough significance to be included in future global fits. Similarly, the  $p_T$  reach of most processes is increased.

## 4 Dijets

The first dijet data from CMS were binned in dijet pseudorapidity,  $\eta_{\text{dijet}}$ , defined as half the sum of the pseudorapidities of the leading and subleading jets, the two hardest (highest  $p_T$ ) jets in the event. It was seen that the dependence of the normalized dijet distribution tracks the  $x$  dependence of the nPDFs. Because of the high  $p_T$  scales,  $p_T > 120$  GeV for the leading jet and  $p_T > 30$  GeV for the subleading jet, at  $\sqrt{s_{NN}} = 5.02$  TeV, with  $\eta_{\text{dijet}} < 0$  in the laboratory frame, the EMC region,  $x > 0.3$ , is probed while, at forward  $\eta_{\text{dijet}}$ , the antishadowing region,  $0.03 < x < 0.3$ , is studied.

In Ref. [2], the CMS  $p_T$  integrated dijet results [17] were compared to two calculations: the CT10 proton PDFs [18] alone and CT10 with EPS09 NLO. When EPS09 NLO was included, the ratio data/EPS09 was within the uncertainty of the nPDF sets while the same ratio with CT10 alone shows significant discrepancies [19].

CMS has recently published a more thorough analysis of these data [21]. The ratio  $pPb/pp$  was given in five bins for the average  $p_T$  of the two jets in the dijet:  $55 < p_T^{\text{ave}} < 75$  GeV;

$75 < p_T^{\text{ave}} < 95$  GeV;  $95 < p_T^{\text{ave}} < 115$  GeV;  $115 < p_T^{\text{ave}} < 150$  GeV; and  $p_T^{\text{ave}} > 150$  GeV and compared to different nPDF sets available before the LHC  $p$ +Pb runs. (Note that these ratios were not directly available for the EPS09 global analysis, only the forward-to-backward pseudorapidity ratio could be used because the  $p$ + $p$  data at 5 TeV were taken only after the 2012  $p$ +Pb run at the same energy.) While none of these data sets probe the shadowing region deeply, because gluons dominate jet production, these data provide the greatest insight into the nuclear gluon distribution in the range  $0.003 < x < 1$  at the highest  $p_T$  scales so far available. This is indeed a great advance because nuclear deep-inelastic scattering can probe gluon distributions only indirectly through their scale evolution and other, lower mass probes of the nuclear gluon density, such as quarkonium, suffer from uncertainties regarding the production mechanism and the relative importance of other cold nuclear matter effects.

While EPS09 still gives a better description of the CMS data than either DSSZ [22] or nCTEQ, EPPS16, which benefited from a global analysis including the  $p_T$ -integrated dijet data [17], gives a superior result to EPS09 compared to the results in different  $p_T$  intervals.

## 5 Gauge Bosons

Massive gauge boson production also provides new and important insight into the charged parton distributions in nuclei, including any differences in the up and down sea quarks, especially for  $W^\pm$  production and the corresponding charge asymmetry. Heretofore, only Drell-Yan data in fixed-target experiments were available to probe this difference. While the scale probed is somewhat smaller than that reached by the dijet data, the lower minimum  $p_T$  required for  $W \rightarrow l\nu_l$  decays, allows these measurements to probe lower values of  $x$ . While the 5.02 TeV data for  $W^\pm$  [14] and  $Z^0$  production [15] were used in the EPPS16 global analysis, the new  $W^\pm$  measurements at 8.16 TeV [23] showed that EPPS16 gives a better description of these data than older sets like nCTEQ that have not yet been updated with the LHC data to guide them.

## 6 Top Quarks

Top quark production in  $p$ +Pb collisions, the most massive, highest scale probe so far for these collisions, was explored in a feasibility study by d'Enterria *et al.* [24] and also presented in Ref. [3]. The measurement was carried out by CMS and reported in the lepton + jet channels:  $l$ +jets,  $\mu$ +jets, and  $e$ +jets in Ref. [25]. So far, only a total cross section in the available phase space can be reported. Given the shorter run time for  $p$ +Pb compared to  $p$ + $p$ , the uncertainties on the data are significantly larger for  $p$ +Pb relative to  $p$ + $p$ . The uncertainties on the predicted cross sections are also larger since the nPDF uncertainties must also be taken into account. The additional sets in EPPS16 relative to EPS09 results in the largest uncertainty band for this set. Better constraints on the gluon nPDF will help reduce these uncertainties in the future. In addition, higher statistics, either at the LHC or a future circular collider, will make it possible to bin the data in different kinematic regions, making it possible to compare to predictions such as those shown in Fig. 3.

## 7 Summary

With  $p$ +Pb collisions at the LHC, the study of perturbative probes of cold nuclear matter in these collisions has entered a new era. High statistics studies of quarkonium and heavy flavors are available to probe the low  $x$  and moderate  $Q^2$  region while high  $p_T$  dijets offer the first clean probe of nuclear gluon PDFs. Gauge boson measurements are now mature enough to distinguish between nPDF sets and separate nuclear effects on individual parton densities than previously possible. These measurements, along with the first observations of top quark production in  $p$ +Pb collisions, show that the parton distributions in nuclei are modified at every scale probed so far.

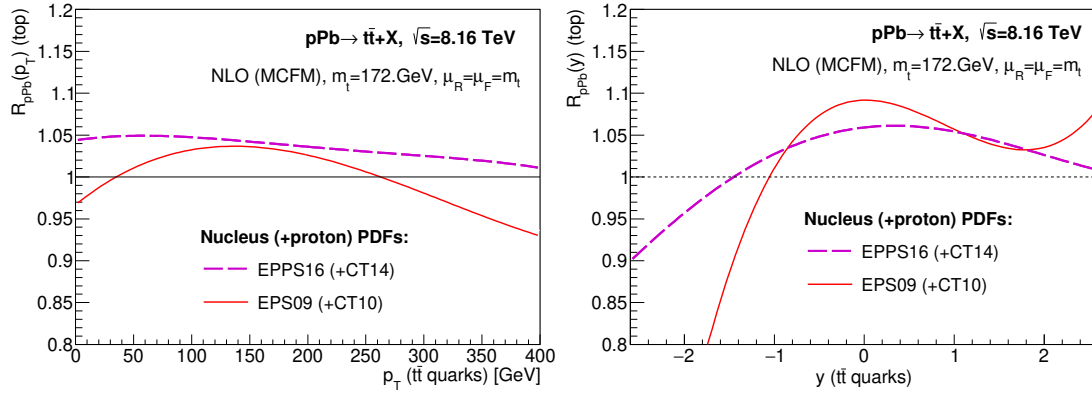


Figure 3 – Nuclear modification factor as a function of  $p_T$  (left) and rapidity (right) for  $t\bar{t}$  production in the  $\ell$ +jets channel at  $\sqrt{s_{NN}} = 8.16$  TeV. Taken from Ref. [3].

## Acknowledgments

I thank all my coauthors of Refs. [1–3] for their collegial collaboration over the years. I also thank the organizers for their kind invitation. This work was performed under the auspices of the U.S. Department of Energy by Lawrence Livermore National Laboratory under Contract DE-AC52-07NA27344 and supported by the U.S. Department of Energy, Office of Science, Office of Nuclear Physics (Nuclear Theory) under contract number DE-SC-0004014.

## References

1. J. Albacete *et al.*, *Int. J. Mod. Phys. E* **22**, 1330007 (2013).
2. J. Albacete *et al.*, *Int. J. Mod. Phys. E* **25**, 1630005 (2016).
3. J. Albacete *et al.*, *Nucl. Phys. A* **972**, 18 (2018).
4. W. Shaikh [ALICE Collaboration], arXiv:1907.00153 [hep-ex].
5. R. Aaij *et al.* [LHCb Collaboration], *JHEP* **1811**, 194 (2018).
6. R. Aaij *et al.* [LHCb Collaboration], *Phys. Lett. B* **774**, 159 (2017).
7. R. Aaij *et al.* [LHCb Collaboration], *Phys. Rev. D* **99**, 052011 (2019).
8. K. J. Eskola, P. Paakkinen, H. Paukkunen and C. A. Salgado, *Eur. Phys. J. C* **77**, 163 (2017).
9. R. Vogt, *Phys. Rev. C* **92**, 034909 (2015).
10. J. P. Lansberg and H. S. Shao, *Eur. Phys. J. C* **77**, 1 (2017).
11. K. Kovarik *et al.*, *Phys. Rev. D* **93**, 085037 (2016).
12. F. Arleo and S. Peigné, *Phys. Rev. Lett.* **189**, 122301 (2012), *JHEP* **1303**, 122 (2013).
13. G. Br, *et al.*, *PoS HardProbes 2018*, 045 (2019).
14. V. Khachatryan *et al.* [CMS Collaboration], *Phys. Lett. B* **750**, 365 (2015).
15. V. Khachatryan *et al.* [CMS Collaboration], *Phys. Lett. B* **759**, 36 (2016).
16. G. Aad *et al.* [ATLAS Collaboration], *Phys. Rev. C* **92**, 044915 (2015).
17. S. Chatrchyan *et al.* [CMS Collaboration], *Eur. Phys. J. C* **74**, 2951 (2014).
18. H. L. Lai *et al.*, *Phys. Rev. D* **82**, 074024 (2010).
19. K. J. Eskola, H. Paukkunen and C. A. Salgado, *JHEP* **1310**, 213 (2013).
20. K. J. Eskola, H. Paukkunen and C. A. Salgado, *JHEP* **0904**, 065 (2009).
21. A. M. Sirunyan *et al.* [CMS Collaboration], *Phys. Rev. Lett.* **121**, 062002 (2018).
22. D. de Florian, R. Sassot, P. Zurita and M. Stratmann, *Phys. Rev. D* **85**, 074028 (2012).
23. A. M. Sirunyan *et al.* [CMS Collaboration], arxiv:1905.01486 [hep-ex].
24. D. d’Enterria, K. Krajczár and H. Paukkunen, *Phys. Lett. B* **746**, 64 (2015).
25. A. M. Sirunyan *et al.* [CMS Collaboration], *Phys. Rev. Lett.* **119**, 242001 (2017).